Neuropsychologia 128 (2019) 178–186

Contents lists available at ScienceDirect

Neuropsychologia

journal homepage: www.elsevier.com/locate/neuropsychologia

More than blindsight: Case report of a child with extraordinary visual capacity following perinatal bilateral occipital lobe injury

Inaki-Carril Mundinano[a], Juan Chen[b], Mitchell de Souza[a], Marc G. Sarossy[c], Marc F. Joanisse[b,d], Melvyn A. Goodale[b], James A. Bourne[a,*]

[a] Australian Regenerative Medicine Institute, Monash University, Victoria 3800, Australia
[b] The Brain and Mind Institute, The University of Western Ontario, London, ON, Canada
[c] Centre for Eye Research Australia, Royal Victorian Eye and Ear Hospital, Melbourne, Victoria, Australia
[d] Department of Psychology, The University of Western Ontario, London, ON, Canada

ARTICLE INFO

Keywords:
Pulvinar
Visual cortex
MRI
Scotoma
Visual field
MCAD
Cortical injury

ABSTRACT

Injury to the primary visual cortex (V1, striate cortex) and the geniculostriate pathway in adults results in cortical blindness, abolishing conscious visual perception. Early studies by Larry Weiskrantz and colleagues demonstrated that some patients with an occipital-lobe injury exhibited a degree of unconscious vision and visually-guided behaviour within the blind field. A more recent focus has been the observed phenomenon whereby early-life injury to V1 often results in the preservation of visual perception in both monkeys and humans. These findings initiated a concerted effort on multiple fronts, including nonhuman primate studies, to uncover the neural substrate/s of the spared conscious vision. In both adult and early-life cases of V1 injury, evidence suggests the involvement of the Middle Temporal area (MT) of the extrastriate visual cortex, which is an integral component area of the dorsal stream and is also associated with visually-guided behaviors. Because of the limited number of early-life V1 injury cases for humans, the outstanding question in the field is what secondary visual pathways are responsible for this extraordinary capacity? Here we report for the first time a case of a child (B.I.) who suffered a bilateral occipital-lobe injury in the first two weeks postnatally due to medium-chain acyl-Co-A dehydrogenase deficiency. At 6 years of age, B.I. underwent a battery of neurophysiological tests, as well as structural and diffusion MRI and ophthalmic examination at 7 years. Despite the extensive bilateral occipital cortical damage, B.I. has extensive conscious visual abilities, is not blind, and can use vision to navigate his environment. Furthermore, unlike blindsight patients, he can readily and consciously identify happy and neutral faces and colors, tasks associated with ventral stream processing. These findings suggest significant rerouting of visual information. To identify the putative visual pathway/s responsible for this ability, MRI tractography of secondary visual pathways connecting MT with the lateral geniculate nucleus (LGN) and the inferior pulvinar (PI) were analysed. Results revealed an increased PI-MT pathway in the left hemisphere, suggesting that this pulvinar relay could be the neural pathway affording the preserved visual capacity following an early-life lesion of V1. These findings corroborate anatomical evidence from monkeys showing an enhanced PI-MT pathway following an early-life lesion of V1, compared to adults.

1. Introduction

In primates, including humans, the perception of visual information is mediated by a pathway from the retina to the primary visual cortex (V1, striate cortex) via the lateral geniculate nucleus (LGN) (Felleman and Van Essen, 1991). From V1, the visual information is distributed to extrastriate cortical areas following two parallel pathways: the dorsal visual stream, which progresses to the parietal cortex via the middle temporal area (MT) and mediates visually guided behaviors; and, the ventral visual stream, which reaches the temporal cortex via areas V2, V3 and V4, and mediates object perception (Goodale and Milner, 1992).

Damage to V1, therefore, results in disconnection of the flow of visual information resulting in a blind spot or 'scotoma' in the visual field. However, early work pioneered by Larry Weiskrantz and colleagues in the 1970's demonstrated that a patient with a V1 injury was able to detect an object in the scotoma well above chance (Weiskrantz, 1986). Weiskrantz called this phenomenon, whereby a patient's behaviour was reliably controlled by a visual stimulus the patient could not

* Corresponding author.
E-mail address: james.bourne@monash.edu (J.A. Bourne).

https://doi.org/10.1016/j.neuropsychologia.2017.11.017
Received 24 July 2017; Received in revised form 26 September 2017; Accepted 12 November 2017
Available online 13 November 2017
0028-3932/

see, 'blindsight'. Subsequent studies in humans (Barbur et al., 1980; Fendrich et al., 1992; Goebel et al., 2001; Innocenti et al., 1999) and monkeys (Cowey and Stoerig, 1997; Innocenti et al., 1999; Schmid et al., 2010a, 2010b) have revealed much information on the visual capacity associated with blindsight, demonstrating a remarkable range of residual visual abilities. Much work continues today exploring these spared visual capacities in both monkeys and man (Bridge et al., 2008; Yu et al., 2013).

Identifying the neural substrate responsible for the phenomenon has been slightly more contentious but most studies in humans (Ajina et al., 2015a, 2015b; Bridge et al., 2010) and monkeys (Rosa et al., 2000; Schmid et al., 2010a, 2010b) report that neurons in MT of the extrastriate cortex, involved in motion processing, respond to a certain degree in the absence of V1. Furthermore, area MT has been demonstrated to respond to global motion differently in patients following a lesion of V1 in adulthood, where coherence-related activity was more representative of V1 (Tamietto and Morrone, 2016), suggesting that it can take up specific functions of V1 in its absence. This has led researchers to develop hypotheses around alternative visual pathways that bypass V1, including a disynaptic pathway through the K layers of the lateral geniculate nucleus (LGN) (Sincich et al., 2004) and via the medial subdivision of the inferior pulvinar (PIm) (Bridge et al., 2016; Warner et al., 2010). The majority of evidence points towards the LGN being the neural substrate following an adult lesion of V1 (Bridge et al., 2016; Schmid et al., 2010a, 2010b) but a role for the retinorecipient pulvinar cannot be discounted (Gross, 1991; Rodman et al., 1990).

A consideration that has received little attention and needs further exploration is the age-associated visual capacity following a lesion to V1. Few studies to date have focussed on perinatal V1 injury. Instead, most comprehensive studies have examined the residual visual abilities of adult humans and monkeys that received a V1 injury. This likely emerged as a consequence of the early work by Lambert and colleagues (Lambert et al., 1987) who studied 30 infants with cortical blindness and concluded that they had poor visual outcomes, which they attributed to premature birth. Evidence does exist from patient M.S., however, who received a bilateral lesion to V1 in early life and shows a superior visual capacity to individuals with a similar injury received later in life (Innocenti et al., 1999). Indeed, in some tasks, M.S.'s performance matched that of children of her age. Other patients are also examples of early-life unilateral and bilateral occipital lobe injury who have near normal visual ability (Werth, 2006). One of the most studied cases is patient G.Y., who sustained unilateral V1 damage at the age of 8 years old. G.Y showed remarkable residual visual capacities and has become a representative case of blindsight (Barbur et al., 1980; Bridge et al., 2008; Weiskrantz, 1996). Seminal studies of experimental V1 lesions in macaque monkeys at 5–6 weeks of age determined that monkeys were able to detect stimuli within their scotoma (Moore et al., 1996). As with blindsight, the cortical areas postulated to be responsible for the preserved vision in these cases are the extrastriate areas, including MT which is a visual area known to mature early in humans and monkeys (Bourne and Morrone, 2017; Bourne and Rosa, 2006; Mundinano et al., 2015; Watson et al., 1993), but the pathway/s responsible still remain undetermined.

Here we present the case of a child (B.I.) who received extensive bilateral damage to the occipital cortex within the first two postnatal weeks, but who has an exceptional visual ability. To demonstrate this, we performed an ophthalmological assessment and examined different visual behaviour tasks such as contrast sensitivity, orientation and shape discrimination, color recognition, 2D and 3D object recognition, face discrimination and grasping. Finally, to interrogate which neural pathways might be underpinning his residual visual abilities, we performed structural and diffusion MRI, comparing results with 4 healthy young male controls.

2. Case report

2.1. History

Patient B.I., male, at the age of 9 days old suffered from seizures and neonatal hypoglycemia caused by a medium-chain acyl-Co-A dehydrogenase deficiency (MCAD). MRI studies immediately after the incident revealed normal brain characteristics (gyral pattern consistent with gestational age, the ventricular system was normal, no intracranial haemorrhage, normal parenchymal echogenicity and extra-axial spaces, and normal posterior fossa). A second MRI study 20 days later revealed severe acute ischemic changes, secondary to hypoglycemia, in the bilateral occipitoparietal lobes, optic radiations and splenium of the corpus callosum, with corresponding hypointensity apparent on diffusion coefficient maps. The lesions, involving grey and white matter, were hypointense on T1, hyperintense on T2 structural images. At the age of 4 years and six months, a routine MRI study showed extensive regions of gliosis, and grey and white matter volume loss within the occipital cortex bilaterally. The splenium of the corpus callosum was markedly thinned with high signal noted within the posterolateral margins of the thalami. Marked dilatation of the occipital horns of the lateral ventricles secondary to negative mass effect from the adjacent volume loss was detected, although the ventricular system appeared otherwise normal. The infratentorial brain had a normal appearance. The appearances were the typical for brain injury in the context of hypoglycaemia. No seizure activity has been noted since the initial episode associated with hypoglycemia.

Despite the extensive bilateral visual cortex damage, B. I. is not blind but instead has a remarkable preserved visual capability. He can use vision to navigate his immediate environment without any help, walk down hallways from one room to another and manage stairs on his own, without any apparent difficulty. Further examination of patient B.I. was undertaken at age 6–7 years, including ophthalmological, neuropsychological and MRI examination.

2.2. Visual assessment

Distance visual acuity revealed severe vision impairment for the right eye (sc 6/120, could identify the largest top letter of the Snellen chart from 3 m), while the left eye was classified as blind (sc CF@1m; patient was able to count fingers at 1 m) (Dandona and Dandona, 2006). Optic nerve atrophy was detected as determined by pale discs in both eyes.

Kinetic visual field perimetry was performed with a Goldmann perimeter (Haag-Streit Inc, Bern, Switzerland), as described elsewhere (Quinn et al., 1991). Briefly, B.I.'s position at the perimeter was set adjusting the seat and the chin rest. The non-tested eye was occluded with an eye patch. B.I. was asked to fix centrally and press the response buzzer each time the light stimulus was perceived. The stimulus targets were presented along cardinal meridians from a region of non-seeing to a region of seeing. Patient compliance B.I. was only able to detect the largest and brightest target (V4e) feasible. As responses were difficult to ascertain, B.I.'s eye movement responses rather than buzzer pressing were plotted to indicate detection of a peripheral stimulus and to establish the visual field extent. This method has routinely been used in establishing the visual field in young children (Fig. 1). The right eye had a mild constriction of field to 70° along the horizontal meridian with a normal size blind spot. The left eye had a moderately severe concentric field constriction, measuring 50° along the horizontal meridian. The blind spot could not be plotted for the left eye. More formal field testing was not possible given the poor acuity and age of the patient.

Pattern reversal visual evoked potentials (PVEP) were collected using an Espion E2 (Diagnosys Lowell MA) system via gold cup electrodes at Oz and Fz with a ground electrode at the right lateral canthus. All electrode impedances were checked and were less than 5k ohms.

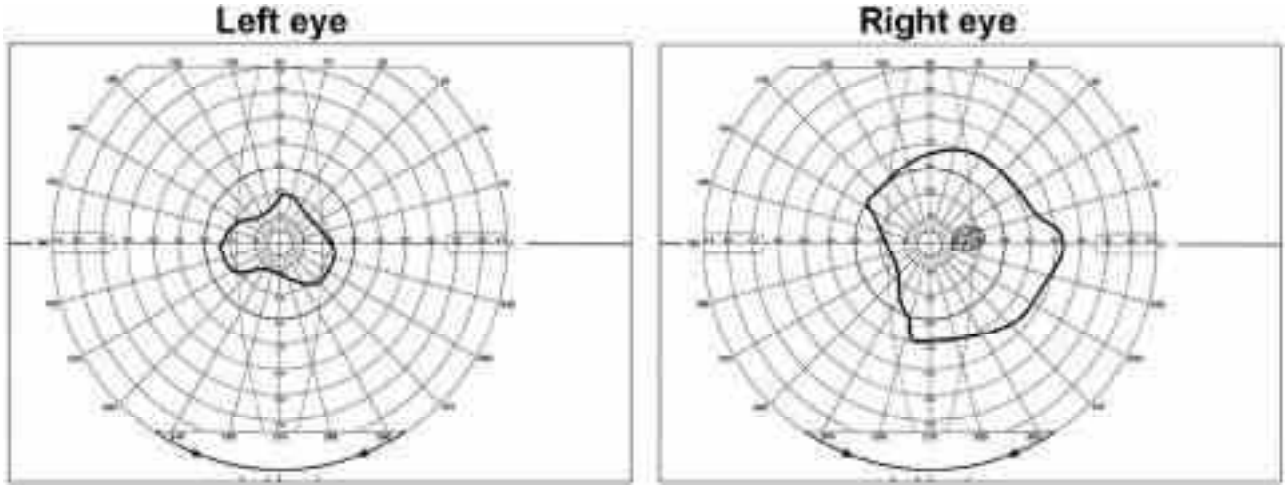

Fig. 1. Goldmann perimetry. Results showing constriction of visual fields for both eyes.

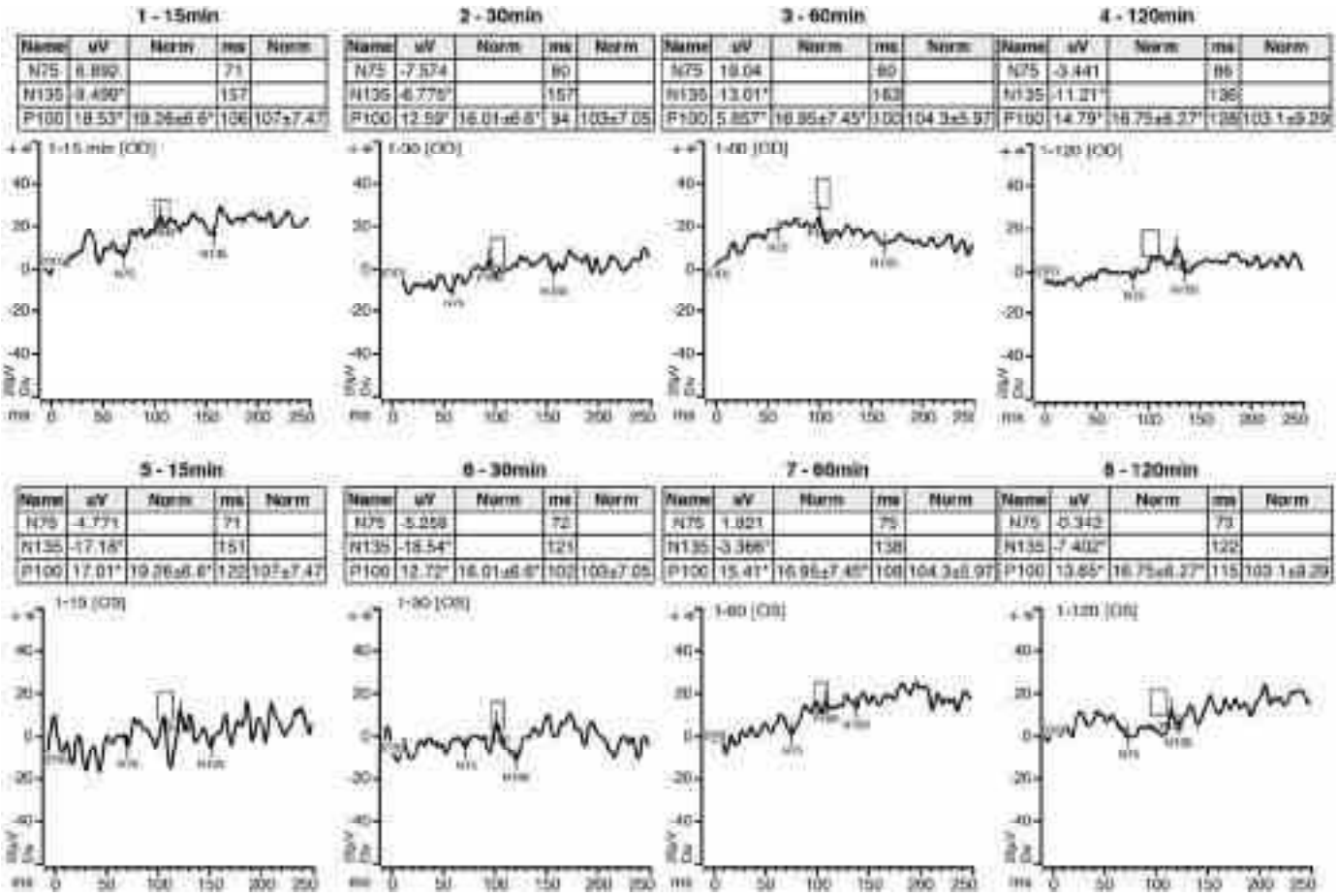

Fig. 2. Pattern visual evoked potential (PVEP). Plots demonstrating lack of responses from both eyes (top row: right eye (OD), bottom row: left eye (OS)) for every stimuli size (15, 30, 60 and 120 min). Boxes in the plots represent the 95% confidence interval from the mean and standard deviation of the normal P100 wave amplitude and implicit time. Tables show amplitude and time values of N75, N135 and P100 waves of patient B.I and normal control P100 wave values.

The test was conducted monocularly and in compliance with the International Society for Clinical Electrophysiology of Vision (ISCEV) standards (Odom et al., 2016). An alternating checkboard pattern stimulus was used at 1 m, performed without refractive correction. Four check sizes were tested (15, 30, 60 and 120 min). There was no measurable response to any of the stimuli from either eye, which is consistent with his diagnosis of visual cortex impairment (Fig. 2).

Ganzfeld flash electroretinograms (ERG) were collected with using an Espion E2 (Diagnosys Lowell MA) using gold cup skin electrodes. This test records the mass electrical activity from the retina when stimulated by various flash intensities in both dark-adapted (scotopic) and light-adapted (photopic) conditions. B.I. was monitored with an inbuilt infrared camera. The test was conducted in accordance with ISCEV standards (Marmor et al., 2004). Electrode impedances were checked and were all under 5k ohms. Photopic dim flash (0.01cds/m2) signals were normal. B.I. was highly photophobic and he found it impossible to

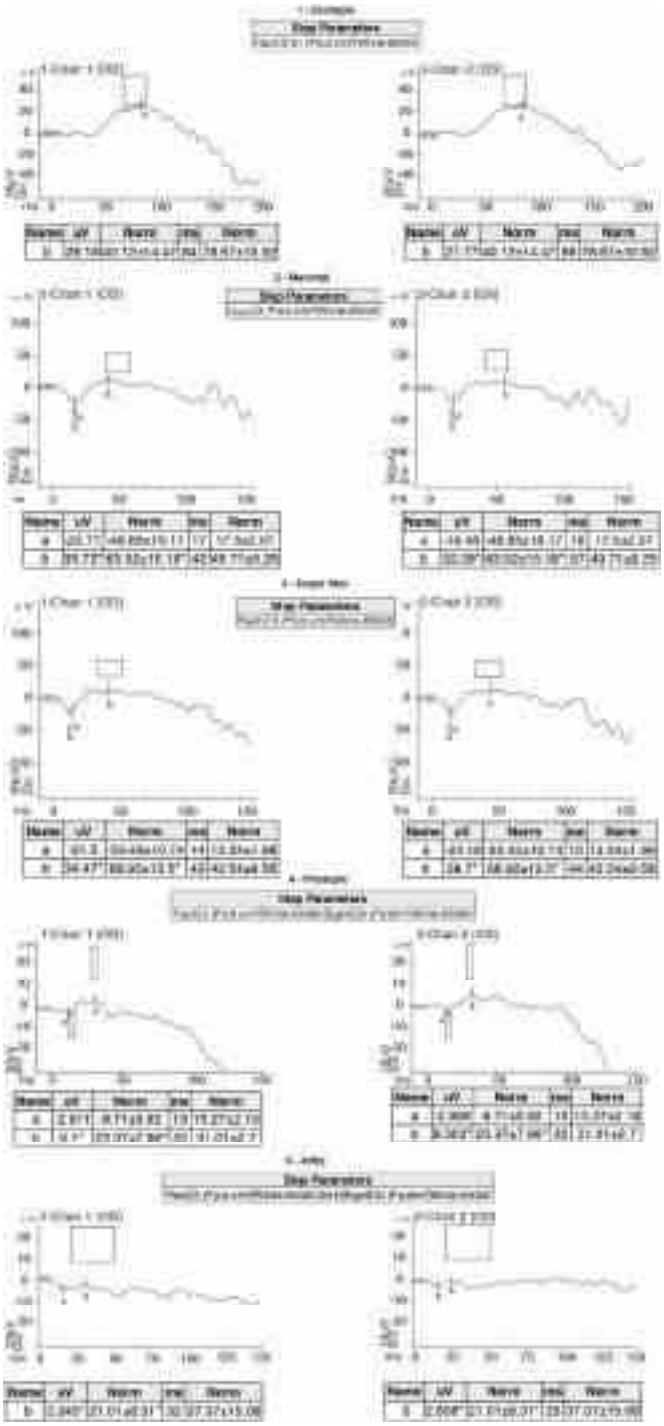

Fig. 3. Electroretinogram results. Plots demonstrating revealing grossly normal retinal function. Boxes in plots represent the 95% confidence interval from the mean and standard deviation of the normal a and b waves amplitude and implicit time values. Tables show amplitude and time values of a and b waves for patient B.I and normal controls (n = 30, aged 18–70).

keep his lids fully open for the remainder of the test sequences. The mixed (3cds/m2) and maximal (10cds/m2) dark-adapted ERG responses were of normal shape but reduced amplitude as a result. The photopic and 30 Hz flicker responses were similarly affected. Given these limitations, the electroretinogram appeared to be grossly normal, not indicating any widespread retinal dysfunction (Fig. 3). Normal values for PVEP and ERG were collected for the laboratory from a cohort of 30 volunteers spanning an age range of 18–70 years of age.

Extraocular muscle function was normal. Ocular alignment analysed by Krimski tests was normal for both eyes (right eye +0.50/−1.75 × 5; left eye plano/1.25 × 155), he also showed clear visual axes.

2.3. Cognitive and visual abilities

In many ways, B.I. appears no different than other children of his age. It was clear that he can use vision to navigate his immediate environment without any help or apparent difficulty. He enjoys playing video games on his tablet, including games where he has to identify and track objects. Outside B.I. can run around and play tag, avoiding trees and other obstacles when doing so. B.I. presented as a cheerful and curious child who was not always enthusiastic about being tested. For this reason, we could not use rigorous psychophysical methods such as staircase procedures. Nevertheless, we were able to obtain assessments of his intellectual performance on standardized tests as well as his performance on a range of tests of visual abilities. The protocols were approved by the University of Western Ontario Ethics Review Board.

2.3.1. Intelligence scale

We tested B.I.'s IQ using two subscales of the *Wechsler Intelligence Scale for Children – Fourth Edition*. For verbal comprehension (we tested vocabulary, comprehension, and similarities), he scored in the 79th percentile for his age group. For working memory (we tested digit span and letter-number sequencing), he scored in the 55th percentile for his age group. In short, he was normal to above normal in his performance on these subscales.

2.3.2. Contrast sensitivity

We were unable to derive a psychometric contrast sensitivity function for B.I. because he was not willing to sit still through the number of trials required to establish thresholds using a traditional psychophysical method, such as a staircase procedure. Therefore, we presented B.I. with Gabor patches of three different spatial frequencies (0.5, 1 and 6 cycles /degree) of varying contrasts (from 0.04 to 1 log units, with a step of 0.04) on a grey background with the same overall luminance as the Gabor patches. The viewing distance was 57 cm and the Gabor patch was 15 cm in diameter. B.I. was asked to report whether or not the patch was present on the grey background. We ran a quasi-formal staircase procedure. For each frequency, we first presented one of the 25 levels of contrast, typically mid-range. If he detected it, then we reduced the contrast; if he did not detect it, then we increased the contrast. We did this for all the three frequencies, but only one staircase for each. He had difficulty detecting the 6 cycles /degree stimuli regardless of contrast. He was able to detect low-contrast stimuli at the two lower spatial frequencies (i.e., 0.5 or 1 cycles/degree). The lowest contrast that he could detect was 0.08 for both the 0.5 cycle/degree and 1 cycle/degree frequency. Note that in this test, and in all the tests described below, B.I. was allowed free viewing, in part because he had difficulty maintaining fixation.

2.3.3. Orientation discrimination

In an informal test, we held up an elongated white rod (2 cm × 12.5 cm) at different orientations and asked B.I. whether we were holding it upright, horizontally, or slanted to the left or right 45°. The viewing distance was approximately 45 cm. Each orientation was presented 5 times in random order for 20 trials with binocular viewing. B.I. performed perfectly on this test.

2.3.4. Shape discrimination

We presented B.I. with pairs of white wooden blocks on a black table top. The 1-cm blocks had the same overall top surface area (25 cm^2) but different aspect ratios (for example, 5 cm × 5 cm, 4.5 cm × 5.56 cm, 4 cm × 6.25 cm, etc.), varying from a square to very elongated rectangular shape (Efron, 1969). The viewing distance was approximately 35 cm. Various combinations of same or different blocks were presented for approximately 20 trials (B.I. grew tired of the testing

after 20 or so trials). He was asked if the two blocks were the same or different. He could reliably make a correct 'different' judgment when the shape differences were large (for example, 5 × 5 cm vs. 3.5 × 7.14 cm), but not when the differences were small (for example, 5 × 5 cm vs. 4 × 6.25 cm).

2.3.5. Color recognition

On a computer screen, we presented B.I. with three different primary colors (red, green and blue) matched for luminance and had him name the color presented on each trial. The color patch was 16 × 16 cm. The viewing distance was 57 cm. B.I. was tested both binocularly and monocularly. In each case, the three colors were presented three times in random order for a total of 9 presentations in each viewing condition. B.I. reported the color accurately for all trials in all viewing conditions.

2.3.6. 2D object recognition

B.I. was required to name objects presented on a computer screen. The objects were depicted in four different formats in separate blocks of trials: full color images, false color images (same as the full color images but with non-diagnostic colors; i.e., a blue banana, a blue basketball, an orange broccoli, a green pumpkin, and a purple bunch of celery, etc.), grey-scale images and line drawings. There were 12 images for each subtype. The longest edge of the images ranged from 12 to 20 cm. The viewing distance was 57 cm. In most cases, B.I. was able to name the object correctly whether it was depicted in full color, grey-scale images, or line drawings. He had some difficulty with some of the smaller images, but even here named them correctly when the picture was enlarged. He named some items incorrectly during the false color block (5 out of the 12 images we showed), indicating again that he can process color information and may rely on both color and shape information to identify an object.

2.3.7. 3D object recognition

We presented B.I. with a series of 3D plastic objects (e.g. lemon, hammer, apple, ball), either with vision alone or haptically with the eyes closed, and asked him to identify each object. The objects themselves (e.g., apple, lemon) or the handle of the object (e.g., hammer) was graspable. The viewing distance was about 35 cm in the visual condition. In the haptic condition, he was allowed to use both hands to feel the objects if needed. Different objects were used in the visual and the haptic trial blocks, 10 objects in each case. B.I. performed perfectly in both cases.

2.3.8. Face discrimination

We carried out two face-discrimination tests in which faces were presented on a computer screen. The images used were selected from the Karolinska Directed Emotional Faces (KDEF) (Lundqvist et al., 1998) (http://www.emotionlab.se/resources/kdef). The viewing distance was approximately 20 cm. In one test, he was presented with two faces (natural with hair) side-by-side which were either the same face or different faces (20 trials in total). Ten individual faces were used in the "same-face" trials; these 10 individuals and another 10 were used in the "different-face" trials. Thus, in total, 20 individual faces were presented. B.I. showed perfect performance when making same/different judgements and even volunteered the gender of the faces, in all cases correctly.

In a separate test, he was asked to report the emotional expression of single faces presented as static pictures. Three facial expressions were used, happy, fearful, and neutral (6 trials in each case). Six individual faces were presented, each having three expressions, for a total of 18 randomized trials. B.I. identified the happy expression in all 6 trials, the neutral expression in all 6 trials, but the fearful expression in only 3 of the 6 trials. B.I. was also presented with videos and asked to mimic the emotional expression shown in the video (6 trials for each expression). The video clips, which were recorded in Dr. Derek Mitchell's Lab at University of Western Ontario, were used with his permission. Again, there were 6 individuals, each having three expressions. He mimicked all the happy expressions correctly, 5 out of the 6 neutral expressions correctly, but only 3 of 6 fearful expressions correctly. His mimicry of 3 of the fearful expressions resembled a neutral expression. B.I.'s performance with the facial expressions is consistent with previous studies showing that children at 7 years of age ((Gao and Maurer, 2009); using a different set of face stimuli) or even at 8–11 years of age ((Mancini et al., 2013); using face stimuli from the same standard set of face stimuli) have more difficulty recognizing fearful than happy expressions. In other words, the profile of B.I.'s performance with happy and fearful expressions appeared to be in the normal range. To strengthen this conclusion, we tested two age-matched children (one girl, 6 years old and 5 months, and one boy, 6 years old and 6 months) with the same facial expression stimuli and procedure that we had used with B.I. The control participants also recognized all happy and neutral expressions, and were able to mimic all the happy and neutral expressions. Like B.I., however, they both had difficulty recognizing and mimicking fearful expressions. One control participant did not recognize 1 of the 6 fearful static faces, and failed to mimic 2 of the fearful face videos correctly. The other control participant did not recognize 2 out of the 6 fearful static faces and did not mimic 2 out of the 6 fearful face videos correctly. Taken together, the earlier studies and the performance of our control participants suggest that B.I.'s ability to recognize and to mimic emotional expressions is essentially normal or near-normal.

2.3.9. Grasping

In an informal session, we presented B.I. with Efron rectangles (i.e. 5 different rectangular objects with same surface area but different widths; the dimensions of the blocks were the same as those used in Section 2.3.4) and asked him to do two things: (1) with his thumb and forefinger estimate the width of the object then pick up the object using the same two fingers, (2) with his thumb and forefinger pick up the object directly. The viewing distance was about 30 cm, and at the beginning of a trial the finger and thumb were approximately 15 cm from the block. In both tests, each object was presented only once. B.I. had difficulty estimating the widths, but had no problem picking up the objects, never fumbling or misdirecting his fingers. Moreover, he never used a small grip to grasp the Efron blocks with a larger width. In other words, his grasping movements seemed perfectly natural. Unfortunately, we were not able to record his kinematic performance systematically because he was uncomfortable wearing the tape used to attach the markers for the motion tracker.

2.4. MRI

2.4.1. Acquisition parameters

MR imaging of patient B.I. was performed on a Siemens Skyra 3T at Monash Biomedical Imaging (Clayton, Australia). The protocols were approved by Monash University Human Research Ethics Committee.

DWI images were acquired using a single shot, twice-refocused spin-echo echo-planar imaging (EPI) sequence, including the following parameters: repetition time (TR)/echo time (TE) = 8800/110 ms; echo train length = 36; Field of view (FOV) = 240 × 240 mm2, acquisition matrix = 96 × 96; slice thickness = 2.5 mm. Diffusion encoding gradients were applied in 60 directions, with a b-value = 3000 s/mm2 with 7 b = 0 volumes. Acquisition time was 15 min. To enable correction for geometric distortions, a b = 0 image was acquired with the same resolution, FOV and readout bandwidth as the DW-image series, but with reversal of the direction of acquisition along the phase-encode (PE) axis for one of the two images. T1-weighted anatomical contrast image was acquired using the magnetization-prepared rapid acquisition gradient echo (MPRAGE) sequence (FOV = 240 × 2256 mm, matrix size = 256 × 240, 192 slices, 1-mm isotropic resolution, TE/TI/TR = 2.07/900/2300 ms, flip angle 9°, 15 min acquisition time).

MRI imaging of healthy control cases (n = 4, all male aged 11, 12,